

OMAE2010-29094

TOWARDS THE IMPROVEMENT OF AUTONOMOUS GLIDER NAVIGATIONAL ACCURACY THROUGH THE USE OF REGIONAL OCEAN MODELS

Ryan N. Smith*

Jonathan Kelly

Robotic Embedded Systems Laboratory
University of Southern California
Los Angeles, California 90089
Email: ryannsmi@usc.edu

Yi Chao

Jet Propulsion Laboratory
California Institute of Technology
4800 Oak Grove Drive
Pasadena, California 91109
Email: yi.chao@jpl.nasa.gov

Burton H. Jones

Department of Marine Biology
University of Southern California
Los Angeles, California 90089
Email: bjones@usc.edu

Gaurav S. Sukhatme

Robotic Embedded Systems Laboratory
University of Southern California
Los Angeles, California 90089
Email: gaurav@usc.edu

ABSTRACT

Autonomous underwater gliders are robust and widely-used ocean sampling platforms that are characterized by their endurance, and are one of the best approaches to gather subsurface data at the appropriate spatial resolution to advance our knowledge of the ocean environment. Gliders generally do not employ sophisticated sensors for underwater localization, but instead dead-reckon between set waypoints. Thus, these vehicles are subject to large positional errors between prescribed and actual surfacing locations. Here, we investigate the implementation of a large-scale, regional ocean model into the trajectory design for autonomous gliders to improve their navigational accuracy. We compute the dead-reckoning error for our Slocum gliders, and compare this to the average positional

error recorded from multiple deployments conducted over the past year. We then compare trajectory plans computed on-board the vehicle during recent deployments to our prediction-based trajectory plans for 140 surfacing occurrences.

INTRODUCTION

Aquatic robots, such as Autonomous Underwater Vehicles (AUVs), and their supporting infrastructure play a major role in the collection of oceanographic data (e.g., [1], [2] and [3]). Autonomous underwater gliders provide one approach to observing ocean processes. Gliders are capable of long-term deployments, remaining out in the ocean for periods of time ranging from several weeks to several months [4]. Although their horizontal speeds are only about 1 km/hr, their longevity, coupled with the use of

*Address all correspondence to this author.

multiple gliders, can compensate by providing an extended temporal and spatial series of observations.

Our research group employs Autonomous Webb Slocum Gliders [5] as mobile sensor platforms in a *coastal* aquatic observing system for the purpose of measuring physical (e.g., temperature, pressure, seismic activity, ocean currents) and chemical (e.g., salinity, nitrate levels, contaminant concentration) phenomena and biological processes (e.g., algal growth and mortality) leading to the development of phytoplankton blooms that have the potential to include harmful algal species, see [6] for further details. As part of this monitoring effort, we have also investigated the use of gliders to track dynamically evolving ocean features, such as phytoplankton blooms and river runoff, [7], [8] and [9]. For this application, and the safe operation of gliders in a high-traffic coastal region, we are interested in increasing the navigational accuracy of the vehicles without adding additional instrumentation that may sacrifice deployment time. To this end, we examine the use of ocean model predictions in the path planning loop to *a priori* account for disturbances caused by ocean currents.

We begin with a brief description of the standard operational procedure for a glider while on deployment. Details on the navigational method and the mission planning and execution are also included. This is followed by a review of the equations of motion for a typical glider. Since the goal of this paper is to increase the navigational accuracy of the vehicle, we present a computation of the dead reckoning error for the vehicle in a still environment (i.e., no environmental disturbances) to provide a baseline error estimation. This baseline error is compared to navigational errors observed during recent deployments. We conclude by examining the navigation and path planning data collected during previous deployments, and compare these to trajectory plans computed by incorporating ocean model predictions. Future experiments are outlined for sea trials with two gliders executing the same mission; one glider utilizing existing planning methods, the other utilizing prediction-based path planning.

STANDARD DEPLOYMENT PROCEDURE

The Slocum glider is a type of AUV designed for long-term ocean sampling and monitoring [10]. It is a 1.5 m (length) by 21.3 cm (diameter), 50 kg, torpedo-shaped vehicle that *flies* through the water by adjusting its volume to



Figure 1. One of USC's autonomous Slocum gliders on deployment off the coast of Catalina Island, CA.

weight ratio and shifting its center of mass. The change in buoyancy generates vertical motion that is translated via two swept wings into a combination of horizontal and vertical motions. A typical glider trajectory is a sequence of dives and climbs that form a vertical sawtooth pattern. Due to this method of locomotion, gliders are not fast moving AUVs, and have operational velocities around 1 km/hr; the same order of magnitude as oceanic currents.

An example mission for a Slocum glider is a maximum depth along with a set of preprogrammed waypoints (W_1, \dots, W_n) that define the mission. As previously mentioned, a typical trajectory is a sawtooth-shaped path. Each down/up cycle is referred to as a yo, and we define a segment to be the composition of multiple yos that begins with a dive from the surface and ends with a surfacing. Each time at the surface, the glider acquires a GPS location. The present location of the vehicle (L) is compared to the next prescribed waypoint in the mission file (W_i), and the on-board computer computes a bearing and range for execution of the next segment of the mission. We will refer to the geographical location at the extent of the computed bearing and range from L to be the aiming point (A_i). The vehicle then dead reckons with the computed bearing and range towards A_i with the intent of surfacing at W_i . The glider operates under closed-loop heading and pitch control only. Thus, the computed bearing is not altered, and the glider must surface to make any corrections or modi-

fications to its trajectory. When the glider completes the computed segment (i.e., determines that it has traveled the requested range at the specified bearing), it surfaces and acquires a GPS fix. Regardless of where the vehicle surfaces, waypoint W_i is determined to be *achieved*. The geographic positional error between the actual surfacing location and W_i is computed, and any error between these two is fully attributed to environmental disturbances (i.e., ocean currents). A depth-averaged current vector is computed, and this is considered when computing the range and bearing to W_{i+1} , the next waypoint in the mission list. Hence, A_i is in general not in the same physical location as W_i . The offset between A_i and W_i is determined by the average velocity and the perceived current experienced during the previous segment.

In general, for large-scale, open-ocean, sampling and monitoring missions, as the gliders were designed for, this type of mission planning and execution is reasonable. Specifically, accuracy and precision are not a top priority, and open-ocean currents are relatively uniform both spatially and temporally. Thus, an estimation of the local currents based on the error observed in the execution of the prior segment is reasonable. However, in a *coastal* region, with the intent to track and monitor an evolving ocean feature, accuracy becomes increasingly important, and current structures in this regime vary significantly both spatially and temporally. It is with these motivations that we investigate the use of 4-D ocean model velocity predictions to aid in the trajectory design process for gliders. In addition to our glider applications, research is active to utilize these vehicles to measure ocean currents in situ [11]. Here the authors address the use of the Conductivity-Temperature-Depth (CTD) and pressure sensors to quantify horizontal and vertical water velocities, respectively, which assists in the dead reckoning capabilities of their vehicles.

GLIDER MODEL

Considerable work has been done on the formulation of the equations of motion and parameter identification for gliders, [12], [13], [14], and Slocum gliders in particular, e.g., [15], [16]. Since we are not directly concerned with altering the low-level controller of the glider, and due to limited space, we do not reproduce these equations of motion, but refer the interested reader to the cited publications and their included references.

Based on a general derivation of the equations of motion for a submerged rigid body presented in [17], we remark that the external force arising from ocean currents can be sufficiently approximated by use of the principle of superposition. Thus, the environmental disturbance is considered additive to the dynamic equations of motion as presented in Eq. (1), where M represents the mass matrix, C accounts for the Coriolis and centripetal terms, D is the drag matrix, g contains the gravity and buoyancy terms, τ accounts for the external forces and control, v is the velocity vector and η is the position vector.

$$M\dot{v} + C(v)v + D(v)v + g(\eta) = \tau + \tau_{current} \quad (1)$$

Combining this with the discussion in the previous section, it is reasonable to assume that we can use the derived equations of motion to compute the path from L to W_i , and then determine A_i by use of ocean current predictions rather than historical observations. An initial investigation into the implementation of this idea is presented in [9]. Here, we use ocean model predictions to determine A_i for each W_i during a deployment of two Slocum gliders in September 2009. The sea trials conducted were a proof of concept experiment, and the results indicated a noticeable ($\sim 50\%$) reduction in the error between the actual surfacing location and the prescribed goal waypoint.

DEAD RECKONING ERROR ESTIMATION

Based on the success of the initial tests presented in [9], we are motivated to further investigate the improvement of navigational capabilities of gliders by use of ocean model predictions. Since a glider depends solely upon dead reckoning for subsurface navigation, the uncertainty in the estimated state will grow without bound. For our applications in the coastal regions of Southern California, we generally require the vehicle to surface frequently (every 3–6 hours), see e.g., [6], [7] and [18]. Since we acquire GPS ground truth frequently, we are able to bound the growth of the state estimation error. This provides a baseline expected error for the assessment of navigational accuracy and precision.

In addition to the GPS receiver, a typical glider carries a PNI TCM2 attitude sensor and a SBE 41CP pressure sensor on-board. The TCM2 incorporates an electronic compass, a three-axis magnetometer and a two-axis tilt sensor, and

is able to provide attitude data at a user-selectable rate of 1 to 30 Hz; heading accuracy is $\pm 1^\circ$ RMS, and roll/pitch accuracy is approximately $\pm 0.2^\circ$ RMS. The SBE measures pressure with an RMS accuracy of 2 decibars, or depth with an RMS accuracy of 2.03 m near the water surface, at a rate of 1 Hz. Together, the TCM2 and the SBE 41CP are the only available sources of navigation information when the glider is submerged.

We establish a baseline estimate of the glider dead reckoning error by simulating a typical mission profile, consisting of a straight segment of eight yos to a maximum depth of 60 m. In the data presented here, we assume a horizontal trajectory distance of 2 km to compare results with the previously analyzed deployment data. We assume that each yo maintains a pitch angle of 26° for diving and surfacing. We remark here that we neither consider measurement error nor mechanical error in realizing a prescribed pitch angle or angle of attack. As presented in Table 1 of [13], experiments with a Slocum glider demonstrate that both the pitch angle and angle of attack vary 3° and 0.6° , respectively, from yo to yo throughout a given mission. Analysis of these statistical parameters for our Slocum gliders is currently under investigation, and incorporation of these errors into the dead reckoning error estimation is ongoing. As in practice, the simulated attitude sensor provides updates at a rate of 5 Hz, and the simulated pressure sensor at a rate of 1 Hz. We also incorporated a simulated, zero-mean, Gaussian noise to each measurement, using the published RMS sensor accuracy values.

We fused the measurements from the simulated attitude sensor and pressure sensor in an unscented Kalman filter (UKF) to estimate the position, attitude and velocity of the vehicle over time [19]. The UKF is a Bayesian filtering algorithm which employs a statistical local linearization procedure to propagate and update the system state. The 10×1 state vector is given in Eqn. (2),

$$\mathbf{x}(t) = [\mathbf{p}^w \bar{q}_b^w \mathbf{v}^b]^T \quad (2)$$

where \mathbf{p}^w is the position of the glider in the world frame, \bar{q}_b^w is the unit quaternion defining the attitude of the glider body relative to the world frame, and \mathbf{v}^b is the velocity of the glider in the body frame. Other studies have investigated the use of Kalman filters for the state estimation of a dead reckoning glider, see e.g., [14]. There, the authors

present a localization algorithm for a glider that utilizes the extended Kalman filter (EKF) for state estimation and propagation. The EKF is an accepted method for creating a navigational filter to manage system model error and perform data fusion from multiple sensors. However, for nonlinear systems, the UKF typically produces significantly more accurate estimates than the EKF, and thus is the reason for its choice in this research.

For our simulation, we assume that the glider follows a nominal linear sawtooth trajectory, and that the vehicle angular rotation rate and linear acceleration are driven by white, zero-mean Gaussian noise processes represented by the vectors $\eta_q(t)$ and $\eta_v(t)$, with covariance matrices \mathbf{Q}_q and \mathbf{Q}_v respectively. The system state evolves in continuous time according to Eqns. (3) - (5),

$$\dot{\mathbf{p}}^w(t) = \mathbf{C}(\bar{q}_b^w(t)) \mathbf{v}^b(t) \quad (3)$$

$$\dot{\bar{q}}_b^w(t) = \frac{1}{2} \Omega(\eta_q(t)) \bar{q}_b^w(t) \quad (4)$$

$$\dot{\mathbf{v}}^b(t) = \eta_v(t) \quad (5)$$

where $\mathbf{C}(\bar{q}_b^w(t))$ is the direction cosine matrix corresponding to the unit quaternion $\bar{q}_b^w(t)$, and $\Omega(\eta_q(t))$ is the quaternion kinematic matrix which relates the rate of change of the orientation quaternion to the body frame angular velocity [20]. We use a continuous-discrete formulation of the UKF, in which the state is propagated forward in time using a fourth-order Runge-Kutta integration of Eqns. (3)–(5). Measurement updates occur at discrete time steps.

The results from two simulation trials are shown in Figs. 2 - 4. Note that by the nature of dead reckoning navigation, the positioning error will grow without bound, as no absolute positioning information is available until the glider surfaces and obtains a GPS fix. For the first simulation, we assume that the glider purely dead reckons using only the on-board attitude sensor. The results of this simulation are presented in Fig. 2, where we display a downward looking view of a 2 km trajectory (blue line) and indicate the 3-sigma uncertainties at the midway point (1 km) and at the terminus of the trajectory by the dashed red ellipses. The small blue circles in Fig. 2 represent the center of the covariance (i.e., the mean). In this scenario, we estimate that the 3-sigma dead reckoning error over this 2 km trajectory is an ellipsoid that has a semi-major axis of 582.9 m, a semi-minor axis of 393.6 m, and an area just larger

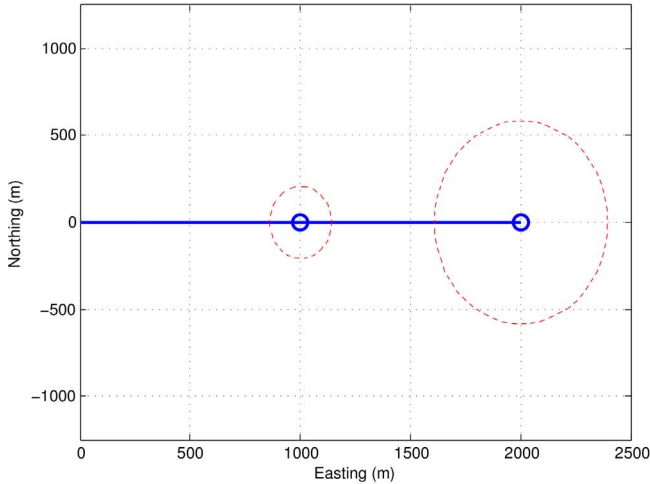


Figure 2. Downward looking view of the glider trajectory (blue line) and the 3-sigma uncertainties of the surfacing location (dashed red ellipses) at a distance of 1 km and 2 km along the trajectory. The small blue (solid) circles represent the center of the covariance (i.e., the mean).

than $720,000 \text{ m}^2$. We see that in Fig. 2, the estimated navigational uncertainty corresponds roughly to a 600 m error, in the worst case. Note also that this error is estimated to occur in similar magnitude in both the long- and cross-track directions. For the data presented in Figs. 3 and 4, we utilize both the attitude sensor and the pressure sensor in the simulation to compute the error estimations. Figure 3 displays a downward looking view of the 2 km trajectory (blue line) and indicates the 3-sigma uncertainties at 500, 1000, 1500 and 2000 meters. In this scenario, we estimate that the 3-sigma dead reckoning error at the end of the 2 km trajectory is an ellipsoid that has a semi-major axis of 582.6 m, a semi-minor axis of 41.1 m, and an area of about $75,000 \text{ m}^2$. The semi-major and semi-minor axes of the uncertainty ellipsoids at 500, 1000 and 1500 meters are (72.8, 21.1), (206, 29.1) and (378.5, 35.5) meters, respectively. It is interesting to note that by only adding the depth sensor measurements into the simulation, we significantly reduce the overall area of the uncertainty ellipsoid at the terminus of the 2 km trajectory. The majority of the reduction occurred in the along-track direction, and the overall area of the uncertainty ellipsoid was reduced by a factor of almost 10. For the unique sawtooth-shaped trajectory pattern that the glider flies, we note the importance of accurate depth measurements in dead reckoning navigation. Figure 4 depicts a three-dimensional view of the simulated

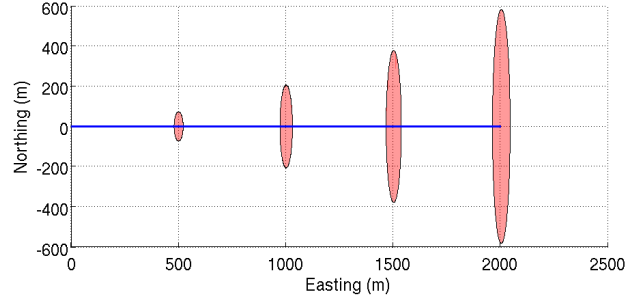


Figure 3. Downward looking view of a 2 km glider trajectory (blue line) with 3-sigma uncertainties at 500, 1000, 1500 and 2000 meters.

trajectory, along with the 3-sigma uncertainties at the surfacing areas closest to 500, 1000, 1500 and 2000 meters along the trajectory. In this figure, we can also see the individual yos that comprise this trajectory segment. Based on the assumption of a fixed pitch angle of 26° for diving and surfacing, the glider is unable to precisely surface at any given distance from its starting location. In Fig. 4, we see that the trajectory does not end at the surface, but slightly below the surface on the downward portion of a new yo. In practice, the glider always ends the trajectory at the surface, and hence is prone to under or overshoot the goal waypoint simply based on the distance from the starting location. In particular, for this example, the glider would have terminated this trajectory before reaching the full 2 km, as executing another full yo would have put the glider further away from the goal waypoint. During deployments, a typical yo (i.e., surface to surface) is approximately 300 m. Thus, if the glider computes that it can surface within 150 m of the goal waypoint, it will not execute an additional yo. This is an interesting feature of the trajectory pattern for autonomous gliders, and can be a hurdle in some path planning applications. As this study is meant to examine the baseline dead reckoning error for our gliders, we omitted this detail in the presented simulation results. Further analysis is planned to account for this trajectory-based artifact.

OCEAN MODEL PREDICTIONS

The predictive tool utilized in this research is the Regional Ocean Model System (ROMS) [21] - a split-explicit, free-surface, topography-following-coordinate oceanic model that is compiled and run by the Jet Propul-

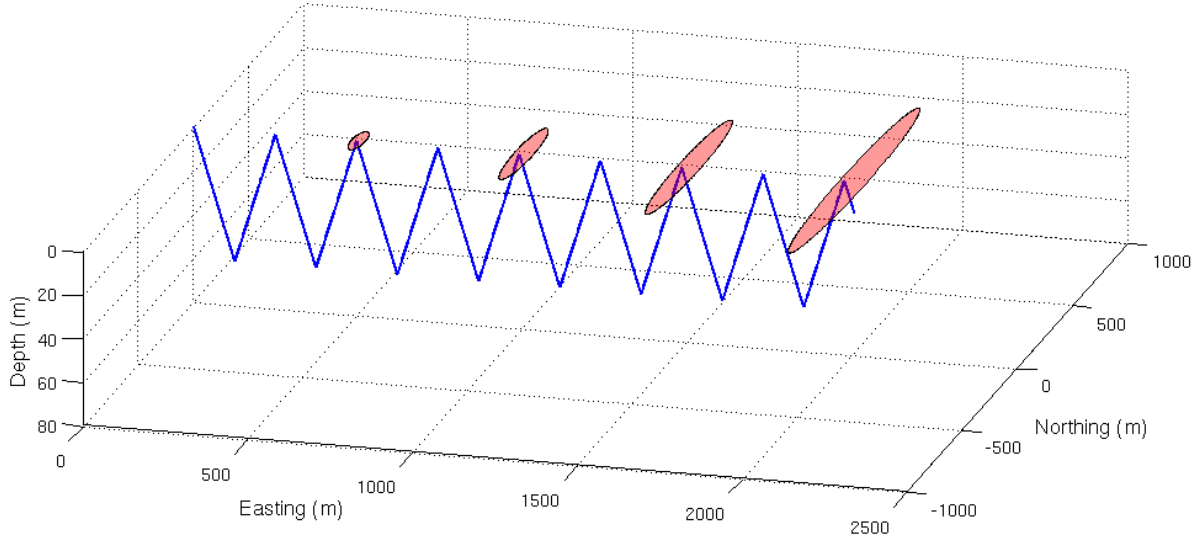


Figure 4. Three-dimensional view of a 2 km glider trajectory (blue line) with 3-sigma (red ellipsoids) uncertainties at approximately 500, 1000, 1500 and 2000 meters.

sion Laboratory (JPL), California Institute of Technology. ROMS is an open-source, ocean model that is widely accepted and supported throughout the oceanographic and modeling communities. Additionally, the model was developed to study ocean processes along the western U.S. coast which is our primary area of study. The JPL provides ROMS hindcasts, nowcasts and hourly forecasts (up to 48 hours) for Southern California, see [22] for more information. The JPL version of ROMS assimilates HF radar surface current measurements, data from moorings, satellite data and any data available from sensor platforms located or operating within the model boundary. The more in situ data that is assimilated into ROMS, the better the predictive skill of the model. Information regarding this version of ROMS and the data assimilation process can be found in [23].

As is the case with any model or simulation, theoretical predictions do not always match what actually occurs in real-life. It is an active area of research to assess and improve the accuracy of regional ocean models, (i.e., JPL ROMS) for use in applications such as ocean monitoring and AUV trajectory design. We have initiated research efforts in these areas, and we continue contributing to the improvement of ROMS through the assimilation of in situ data from glider deployments and static sensor measurements (e.g., [6], [7], [8] and [9]).

For this study, we assume that errors in the ROMS predictions are negligible. This is not a valid assumption, since the model does have inherent errors. However, an overall focus of this research is to develop an innovative toolchain for the path planning and trajectory design of AUVs. By using ocean models and validating our results with sea trials, we not only improve our control algorithms, but offer ground truth for assimilation back into the model that increases model skill over multiple successive iterations.

DATA ANALYSIS

During 2009, we deployed two Slocum gliders that collectively traversed more than 1500 km over a period of more than 100 days. We maintain a database that stores all of the mission information for every deployment. We not only archive the science data collected by the on-board sensors, but we also log mission information, such as surfacing location, destination waypoint, computed range and bearing to each waypoint, average velocity, etc. As noted in [9], from these data we observe a median error between prescribed goal location and actual surfacing location of approximately 1.1 km for an average trajectory length of 2 km. In this section, we consider a subset of the archived navigational data computed on-board the vehicle to compare with computations based on ROMS predictions.

The JPL maintains a complete archive of ROMS model predictions dating back to 2007. Thus, we are able to access the ROMS prediction for the ocean currents that corresponds to the precise time and location of the glider at each surfacing within a given mission. We selected a deployment from April and May 2009, during which two gliders were at sea for 26 days. This dataset provided 140 surfacings for the comparison of navigational data.

Table 1. Statistical analysis of the difference in range (distance) and bearing (heading) from the glider's current location (L) to the aiming point computed using ROMS predictions (A_i^{ROMS}) and to the aiming point computed using the glider's on-board algorithm (A_i^{Glider}).

	Range (m)	Bearing ($^{\circ}$)
Median	200	14.37
Minimum	9.23	-151.04
Maximum	22005	173.82
Mean	1802.25	13.8
Standard Deviation	4684.65	41.2

Table 2. Statistical analysis of the difference in range (distance) and bearing (heading) from the glider's current location (L) to the aiming point computed the glider's on-board algorithm (A_i^{Glider}) and to the actual location of the prescribed waypoint (W_i).

	Range (m)	Bearing ($^{\circ}$)
Median	342.5	-12.97
Minimum	0.2	-43.17
Maximum	1073.7	22
Mean	364.96	-12.69
Standard Deviation	257.05	9.17

Assuming the predicted ocean currents output by ROMS are the currents that the glider will experience, we computed the range and bearing that the glider should use

to successfully dead reckon from its current location to the goal waypoint as defined by the current mission. The procedure for this computation is outlined in [9] and provides a range and bearing for the aiming point A_i^{ROMS} that can be compared to the range and bearing for the aiming point A_i^{Glider} , computed on-board the glider during the deployment. In Table 1 we present the statistical results for the analysis of $A_i^{ROMS} - A_i^{Glider}$ for both range and bearing. Additionally, we provide similar results for $A_i^{Glider} - W_i$ and $A_i^{ROMS} - W_i$ in Tables 2 and 3, respectively.

During the deployment from which the data presented here was gathered, the gliders were set to dive down to a maximum depth of 60 m, which is similar the *deep* trajectory presented in [9], a maximum depth of 80 m. For the deep scenario presented in [9] which used ROMS predictions as the in situ currents, the resulting sea trials gave an error between the prescribed goal location and actual surfacing location of approximately 0.5 km. This corresponds to a 50% reduction in surfacing error from the observed behavior that employed the traditional depth-averaged current estimation method computed on-board the glider. This significant increase in accuracy sparked the motivation to examine the results presented in Tables 1 - 3.

The results in Table 1 display two key trends. First, the range computation utilizing ROMS predictions is consistently greater than that computed on-board the glider. Some discrepancy here is expected because the glider uses the computed average horizontal speed from the last completed segment to compute the range for the subsequent segment, whereas the algorithm incorporating the ROMS predictions

Table 3. Statistical analysis of the difference in range (distance) and bearing (heading) from the glider's current location (L) to the aiming point computed using ROMS predictions (A_i^{ROMS}) and to the actual location of the prescribed waypoint (W_i).

	Range (m)	Bearing ($^{\circ}$)
Median	722.95	1.32
Minimum	0.1	-172.68
Maximum	21998.1	149.78
Mean	2514.76	1.11
Standard Deviation	4403.04	1.32

assumes a constant velocity of 0.75 km/hr for the horizontal speed of the vehicle. This constant speed is the average horizontal velocity of the glider observed over the multiple deployments that we have conducted. However, given that the ROMS algorithm tends to produce larger ranges than the on-board glider controller, this may imply that ROMS current velocity predictions are slightly higher than the actual current velocities. The second note is that the bearing computed by use of ROMS is generally greater than that computed on-board the vehicle. Table 1 also shows that there are times when the computed bearings are in completely opposite directions, implying that the predicted current is probably not the current experienced in situ by the vehicle.

The data presented in Tables 2 and 3 give the statistics for the difference in range and bearing of the computed aiming location and the actual geographic location of the goal waypoint. Table 2 corresponds to the computations made by the glider and Table 3 corresponds to the computations made by use of ROMS predictions. The data presented here further supports the two trends discussed earlier. In addition, we can see a vast difference in the bearing computations carried out by ROMS and the glider. In the case of ROMS computations, we observe a mean bearing difference from the actual bearing to the goal waypoint of 1.11° with a standard deviation of 1.32° . Thus, the bearing computed by ROMS is between -2.85° and 5.07° from the actual bearing to the goal waypoint 99% of the time. On the other hand, for the case of the glider computations we observe a mean bearing difference from the actual bearing to the goal waypoint of -12.69° with a standard deviation of 9.17° . Thus, the bearing computed by the glider is between -40.48° and 14.54° from the actual bearing to the goal waypoint 99% of the time. The larger range in bearing resulting from a greater standard deviation is a result of the glider algorithm assuming that *all* error between actual surfacing location and goal waypoint location is a result of ocean currents. Inevitably, this incorporates the dead reckoning error into the estimation of the ocean current. The problem with this amalgamated error estimation is that in some instances, general ocean currents are more predictable than a glider's dead reckoning error. As a result, this leads to a poor estimation of the actual environmental disturbances and, in turn leads to poor navigational accuracy. By separating the dead reckoning error from the ocean current estimations, it is our intention to increase the

navigational accuracy to the bound of the dead reckoning error concatenated with the estimated error in the chosen predictive ocean model. Depending on the region of interest (i.e., open ocean versus coastal shelf region), estimated error in the predictive model may encourage or prohibit the type of planning examined here. Research is active to further quantify the admissible range of application.

CONCLUSIONS

Based on previous deployment experience with two Slocum gliders, we estimated a median error of 1.1 km between the actual surfacing location and the goal waypoint over an average trajectory length of 2 km. For missions such as feature tracking, as described in [7] and [8], we would like to have better navigational accuracy. By fusing the measurements of simulated attitude and pressure sensors in an unscented Kalman filter, we estimated the position, attitude and velocity of the vehicle over time. Based on the specifications of the instruments on-board the glider, we were also able to propagate the uncertainty of the vehicle's position, attitude and velocity. In this study, we were primarily interested in the uncertainty of the final surfacing location after execution of a 2 km trajectory. From the UKF, we estimated that the three-sigma dead reckoning error for our trajectory is an ellipsoid that has a semi-major axis of 582.6 m, a semi-minor axis of 41.1 m, and an area of about 75,000 m². As seen in Fig. 3, this corresponds to a cross-track error of approximately 600 m, at an angle of 16.7° , in the worst case. Thus, we can reasonably expect that the best achievable accuracy for our Slocum gliders, which dead reckon by use of only an attitude and a pressure sensor, is on the order of 0.5 km for every 2 km traversed. We reiterate that this is roughly half the error that we have seen throughout multiple deployments. However, this estimation matches well with the experimental errors for the deployments that used ROMS predictions for the in situ ocean current rather than the depth-averaged current measurements computed on-board the glider published in [9]; 500 m over a 1.7 km trajectory. Although this may be coincidental, the data provide motivation for further investigation into the incorporation of ROMS predictions into the trajectory design and basic navigation for autonomous gliders. This is an area of active research being carried out in collaboration with the JPL.

Future updates to the simulation include the incorporation of error in the glider's pitch angle, and ending the glider's trajectory at the sea surface into the UKF and the baseline error computations. The current and updated simulation results will aid in the planning and design of future experiments to further assess the validity of ROMS predictions and their incorporation into the path planning for autonomous gliders. For our next deployment, the primary objective will be to provide the same mission file to two different gliders. One glider will operate normally and the other will incorporate ROMS predictions to determine the aiming locations for the goal waypoints. Additionally during this deployment, we will also execute more missions with a single glider navigating by use of ROMS predictions to gather a larger dataset for analysis on the validity of the method and ROMS accuracy. These deployments are planned for January and February 2010.

ACKNOWLEDGMENT

This work was supported in part by the NOAA MERHAB program under grant NA05NOS4781228 and by NSF as part of the Center for Embedded Network Sensing (CENS) under grant CCR-0120778, by NSF grants CNS-0520305 and CNS-0540420, by the ONR MURI program (grants N00014-09-1-1031 and N00014-08-1-0693) by the ONR SoA program and a gift from the Okawa Foundation. The ROMS ocean modeling research described in this publication was carried out by the Jet Propulsion Laboratory (JPL), California Institute of Technology, under a contract with the National Aeronautics and Space Administration (NASA).

REFERENCES

- [1] Godin, M. A., Bellingham, J. G., Rajan, K., Chao, Y., and Leonard, N. E., 2006. "A collaborative portal for ocean observatory control". In Proceedings of the Marine Technology Society / Institute of Electrical and Electronics Engineers Oceans Conference.
- [2] Paley, D., Zhang, F., and Leonard, N., 2008. "Cooperative control for ocean sampling: The glider coordinated control system". *IEEE Transactions on Control Systems Technology*, **16**(4), July, pp. 735–744.
- [3] Whitcomb, L., Yoerger, D., Singh, H., and Howland, J., 1999. "Advances in underwater robot vehicles for deep ocean exploration: Navigation, control, and survey operations". In Proceedings of the Ninth International Symposium of Robotics Research, Springer-Verlag, pp. 439–448.
- [4] Davis, R. E., Ohman, M., Rudnick, D., Sherman, J., and Hodges, B., 2008. "Glider surveillance of physics and biology in the southern california current system". *Limnol. Oceanogr.*, **53**(2), pp. 2151–2168.
- [5] Webb Research Corporation, 2008. <http://www.webbresearch.com/slocum.htm>. viewed May 2008.
- [6] Smith, R. N., Das, J., Heidarsson, H., Pereira, A., Cetinić, I., Darjany, L., Ève Garneau, M., Howard, M. D., Oberg, C., Ragan, M., Schnetzer, A., Seubert, E., Smith, E. C., Stauffer, B. A., Toro-Farmer, G., Caron, D. A., Jones, B. H., and Sukhatme, G. S., 2010. "The Center for Integrated Networked Aquatic PlatformS (CINAPS): Observing and monitoring the southern california bight". *IEEE Robotics and Automation Magazine, Special Issue on Marine Robotics Systems*. To appear March 2010.
- [7] Smith, R. N., Chao, Y., Jones, B. H., Caron, D. A., Li, P. P., and Sukhatme, G. S., 2009. "Trajectory design for autonomous underwater vehicles based on ocean model predictions for feature tracking". In Proceedings of the 7th International Conference on Field and Service Robotics.
- [8] Smith, R. N., Chao, Y., Li, P. P., Caron, D. A., Jones, B. H., and Sukhatme, G. S., 2010. "Planning and implementing trajectories for autonomous underwater vehicles to track evolving ocean processes based on predictions from a regional ocean model". *International Journal of Robotics Research*. Submitted.
- [9] Smith, R. N., Pereira, A. A., Chao, Y., Li, P. P., Caron, D. A., Jones, B. H., and Sukhatme, G. S., 2010. "Autonomous underwater vehicle trajectory design coupled with predictive ocean models: A case study". In Proceedings of the IEEE International Conference on Robotics and Automation. Accepted, to appear.
- [10] Schofield, O., Kohut, J., Aragon, D., Creed, E., Graver, J., Haldman, C., Kerfoot, J., Roarty, H., Jones, C., Webb, D., and Glenn, S., 2007. "Slocum gliders: Robust and ready". *Journal of Field Robotics*, **24**(6), pp. 473–485.
- [11] Merckelbach, L., Briggs, R., Smeed, D., and Griffiths, G., 2008. "Current measurements from autonomous underwater gliders". In Proceedings of

- the IEEE/OES/CMTC Ninth Working Conference on Current Measurement Technology.
- [12] Graver, J. G., 2005. “Underwater gliders: Dynamics, control and design”. PhD thesis, Princeton University.
- [13] Graver, J. G., Bachmayer, R., Leonard, N. E., and Fratantoni, D. M., 2003. “Underwater glider model parameter identification”. In Proceedings of the 13th International Symposium on Unmanned Untethered Submersible Technology.
- [14] Bender, A., Steinberg, D. M., Friedman, A. L., and Williams, S. B., 2008. “Analysis of an autonomous underwater glider”. In Proceedings of the Australasian Conference on Robotics and Automation.
- [15] Leonard, N., and Graver, J., 2001. “Model-based feedback control of autonomous underwater gliders”. *IEEE Journal of Oceanic Engineering, Special Issue on Autonomous Ocean-Sampling Networks*, **26**(4), Oct., pp. 633–645.
- [16] Bhatta, P., and Leonard, N., 2002. “Stabilization and coordination of underwater gliders”. In Proceedings of the 41st IEEE Conference on Decision and Control, Vol. 2, pp. 2081–2086.
- [17] Fossen, T. I., 1994. *Guidance and Control of Ocean Vehicles*. John Wiley & Sons.
- [18] Smith, R. N., Das, J., Heidarsson, H., Pereira, A., Caron, D. A., Jones, B. H., and Sukhatme, G. S., 2009. “Implementation of an embedded sensor network for the coordination of slocum gliders for coastal monitoring and observation”. In WUWNet '09: Proceedings of the Fourth ACM International Workshop on UnderWater Networks, ACM, pp. 1–8.
- [19] Julier, S. J., and Uhlmann, J. K., 2004. “Unscented filtering and nonlinear estimation”. *Proceedings of the IEEE*, **92**(3), March, pp. 401–422.
- [20] Stevens, B. L., and Lewis, F. L., 2003. *Aircraft Control and Simulation*, Second ed. Wiley-Interscience, Oct.
- [21] Shchepetkin, A. F., and McWilliams, J. C., 2005. “The regional oceanic modeling system (ROMS): a split-explicit, free-surface, topography-following-coordinate oceanic model”. *Ocean Modeling*, **9**, pp. 347–404. doi:10.1016/j.ocemod.2004.08.002.
- [22] Q. Vu, 2008. JPL OurOcean portal. <http://ourocean.jpl.nasa.gov/>. viewed February 2009.
- [23] Li, Z., Chao, Y., McWilliams, J. C., and Ide, K., 2008. “A three-dimensional variational data assimilation scheme for the regional ocean modeling system”. *Journal of Atmospheric and Oceanic Technology*, **25**, pp. 2074–2090.